



# 3D RADIATIVE MHD MODELING OF THE SOLAR TRANSITION ZONE AND CORONA

Irina N. Kitiashvili<sup>1</sup>, Viacheslav M. Sadykov<sup>2</sup>, Alexander G. Kosovichev<sup>1,3</sup>, Alan A. Wray<sup>1</sup>

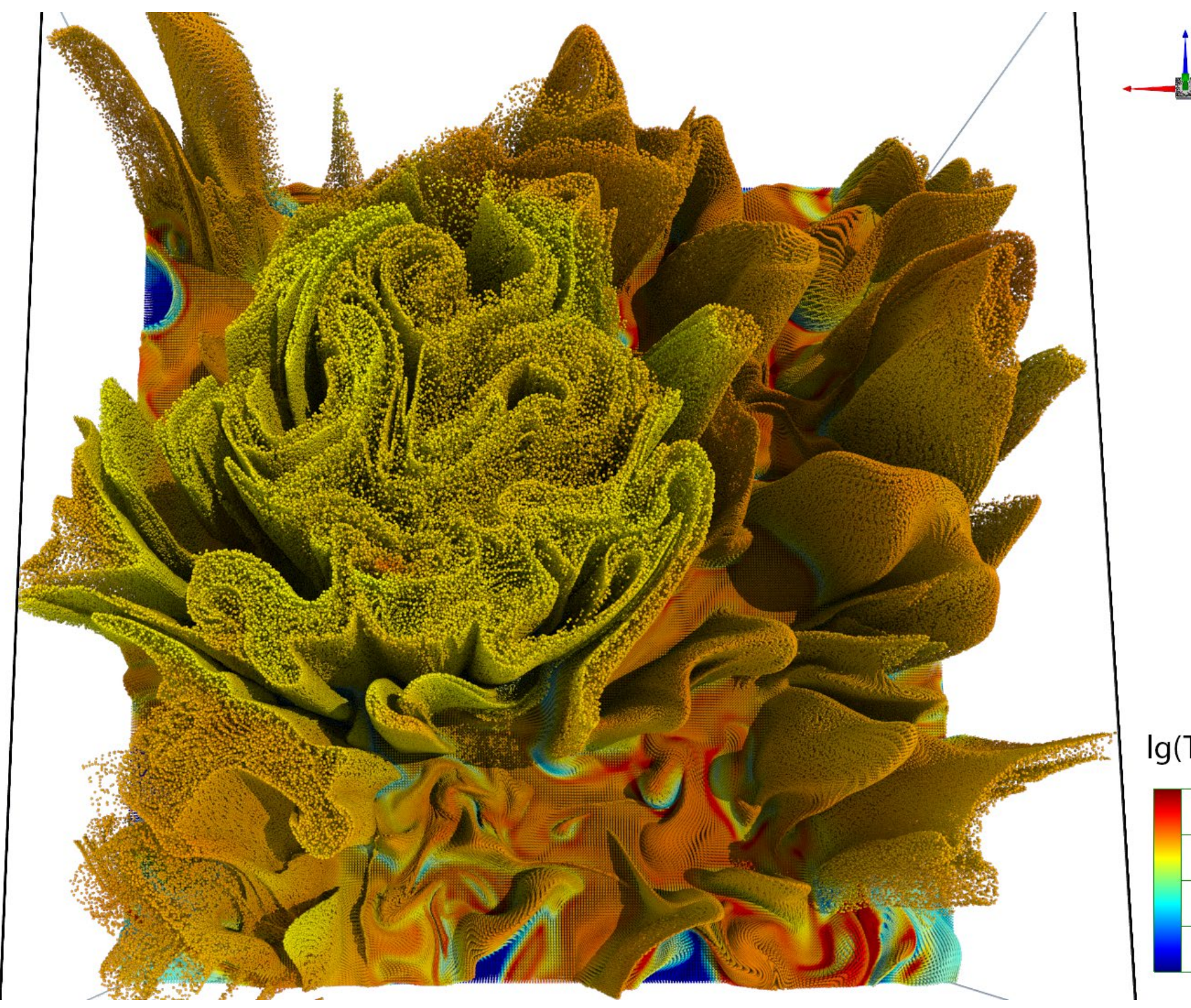
<sup>1</sup>NASA Ames Research Center, <sup>3</sup>Georgia State University, <sup>3</sup>New Jersey Institute of Technology

[Irina.N.Kitiashvili@nasa.gov](mailto:Irina.N.Kitiashvili@nasa.gov)

A variety of dynamical phenomena accompanied by strong thermodynamic and magnetic structural changes are of great interest in studying the solar atmosphere with high spatial and temporal resolutions. Using current computational capabilities, it is possible to model the magnetized solar plasma in different regimes with a high degree of realism. We use 3D radiative MHD models covering all layers from the upper convection zone to the corona to study the fine structure of the solar atmosphere and its dynamics. Realistic 3D radiative MHD modeling of solar magnetoconvection and the atmosphere allows us to generate synthetic observables that directly link the physical properties of the solar plasma to spectroscopic observables. We present 3D MHD simulations of quiet-Sun dynamics that cover the upper layers of the convection zone up to 25Mm above the photosphere. The simulations reveal the formation of self-organized funnel-like dynamical magnetic structures that extend through the chromosphere and corona, spontaneous heating events near the transition zone, and switch-back-like outflows. We calculate a series of synthetic spectropolarimetric imaging data that model observations from different space instruments: HMI and AIA (SDO), SOT (Hinode), and IRIS, and investigate how the observational data are linked to physical processes in the solar atmosphere. In the presentation, we discuss qualitative and quantitative changes in atmospheric structure and dynamics at different layers of the solar atmosphere, properties of acoustic and surface gravity waves, sources of local heating in the chromosphere-corona transition region, formation of shocks, and high-frequency oscillations in the corona, as well as manifestations of these phenomena in the modeled observables.

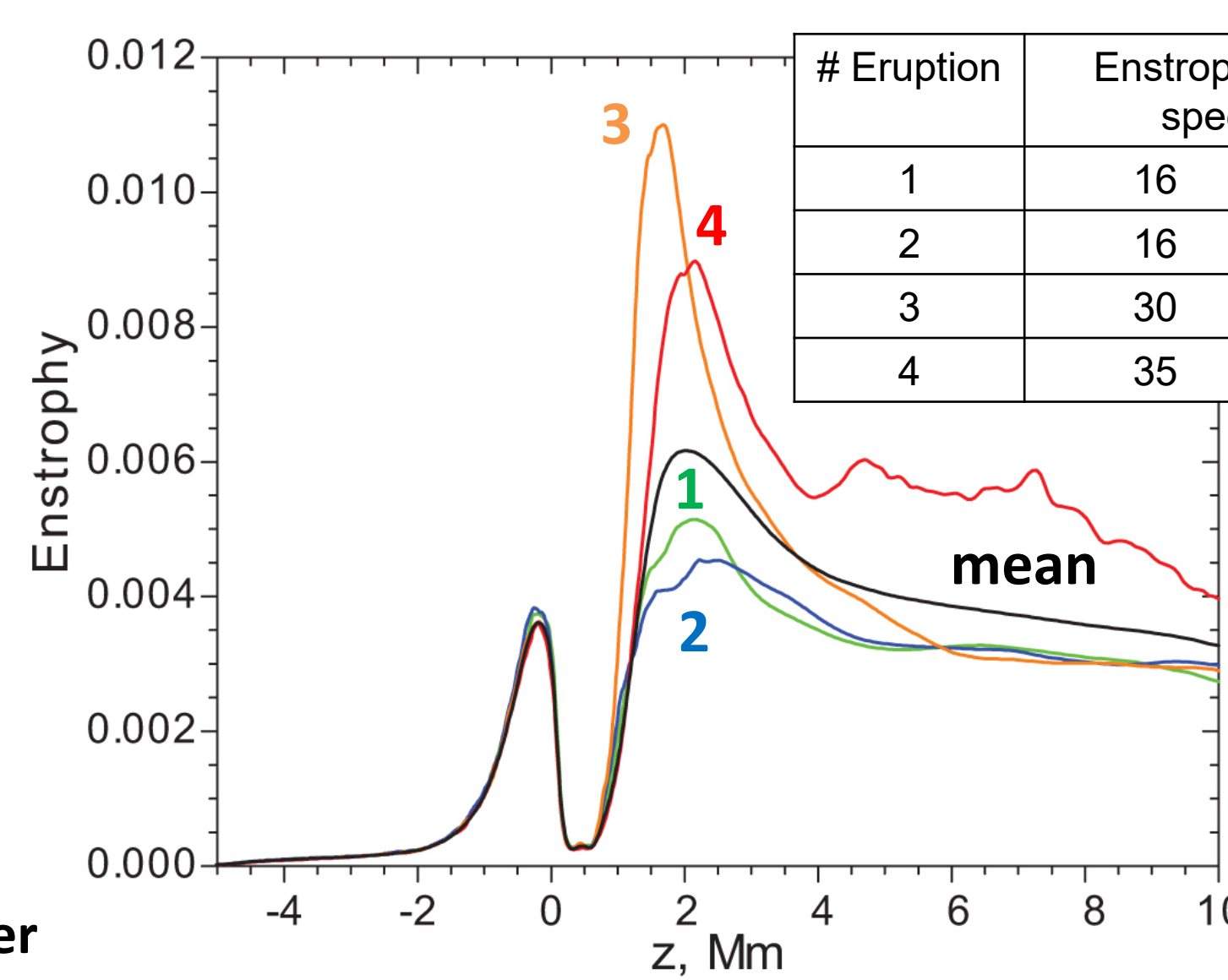
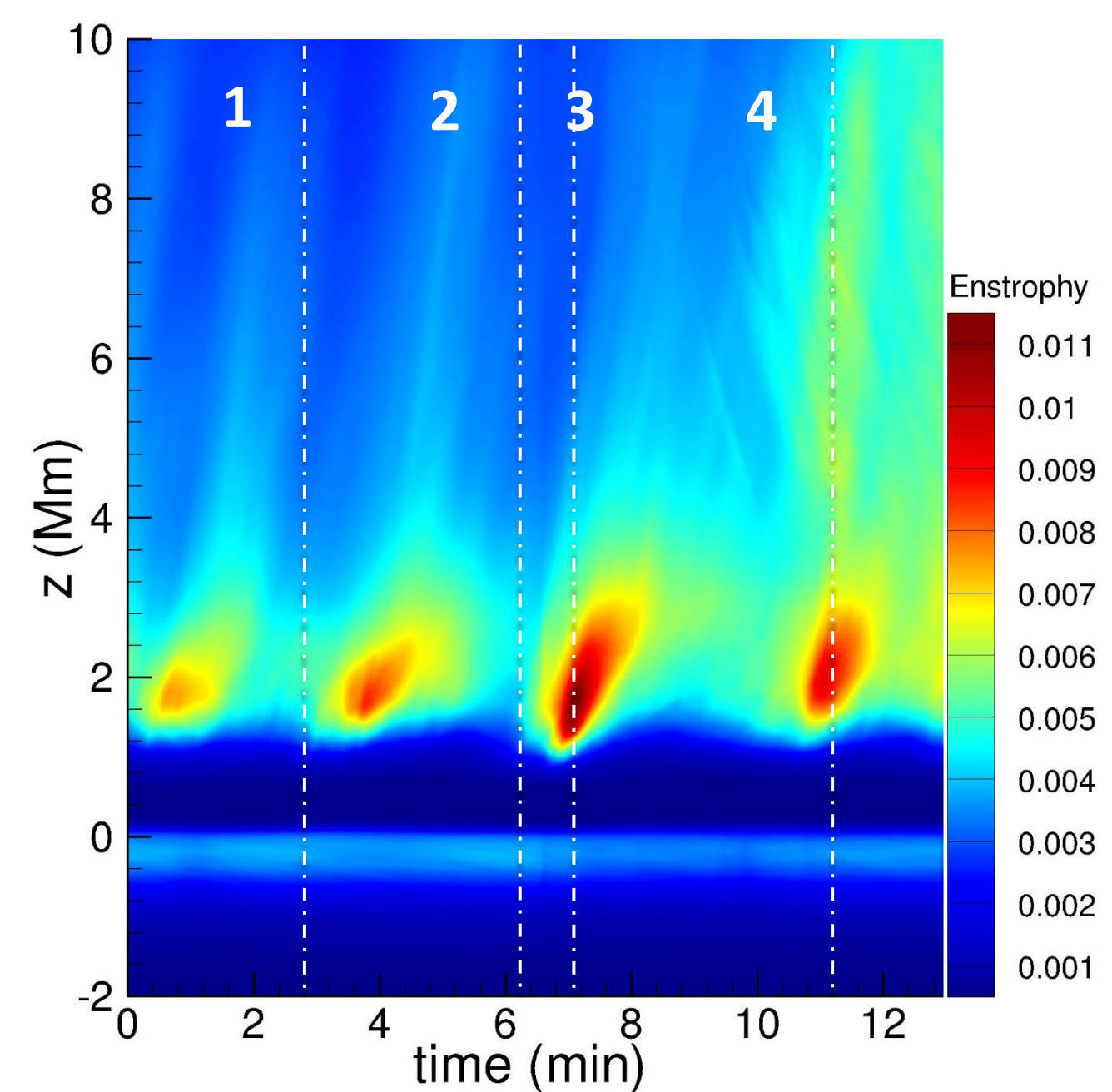
## 'StellarBox' code (Wray et al., 2018)

- ✓ 3D rectangular geometry
- ✓ Fully conservative, Fully compressible
- ✓ Fully coupled radiation solver:
  - LTE using 4 opacity-distribution-function bins
  - Ray-tracing transport by Feautrier method
  - 18 ray angular quadrature
- ✓ Non-ideal (tabular) EOS
- ✓ 4th order Padé spatial discretization
- ✓ 4th order Runge-Kutta time integration
- ✓ Turbulence models:
  - Compressible Smagorinsky model
  - Compressible Dynamics Smagorinsky mode (Germano et al., 1991; Moin et al., 1991)
  - MHD subgrid models (Balarac et al., 2010)
  - DNS+Hyperviscosity approach
- ✓ MPI parallelization (plane and pencil versions)

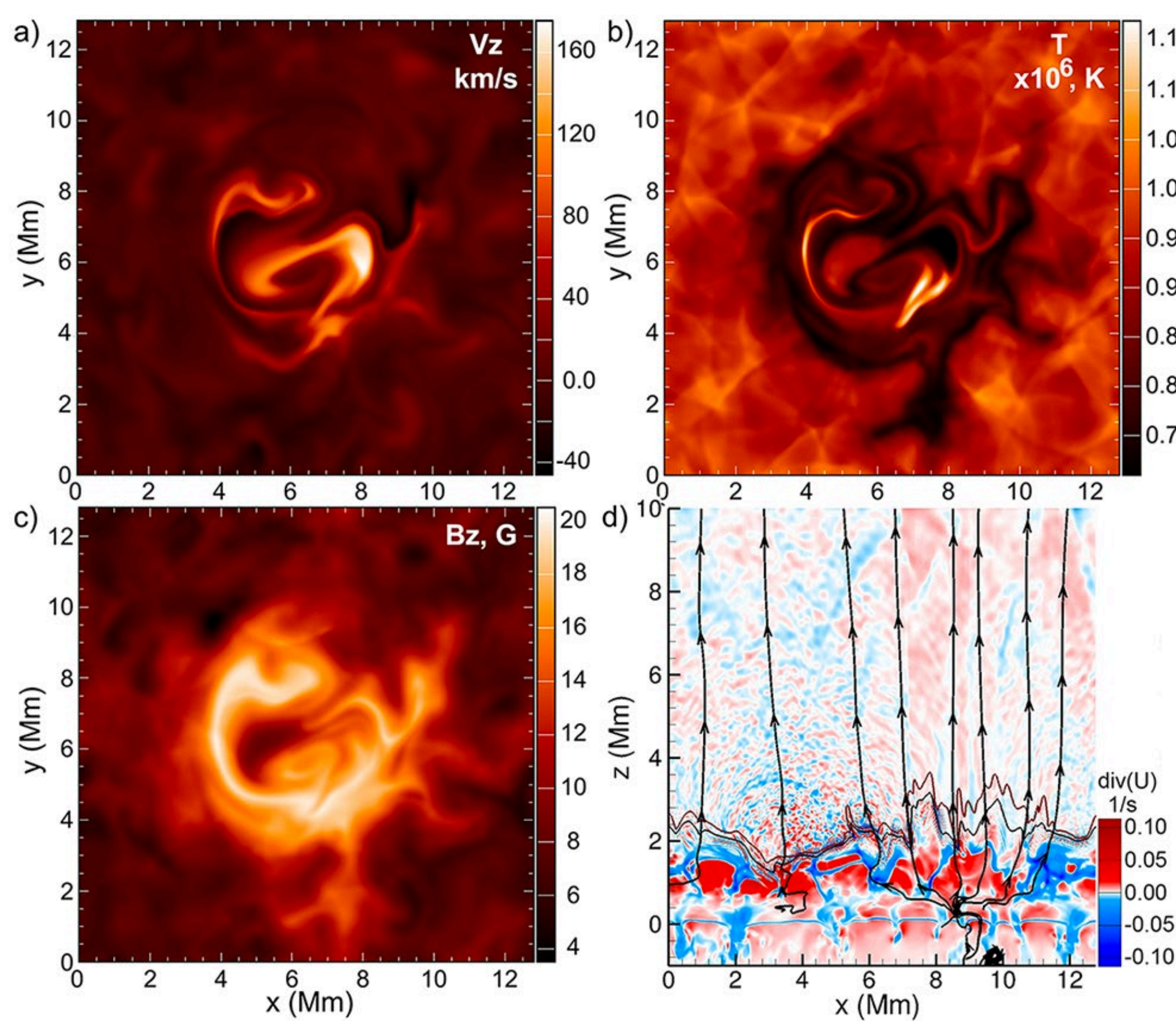
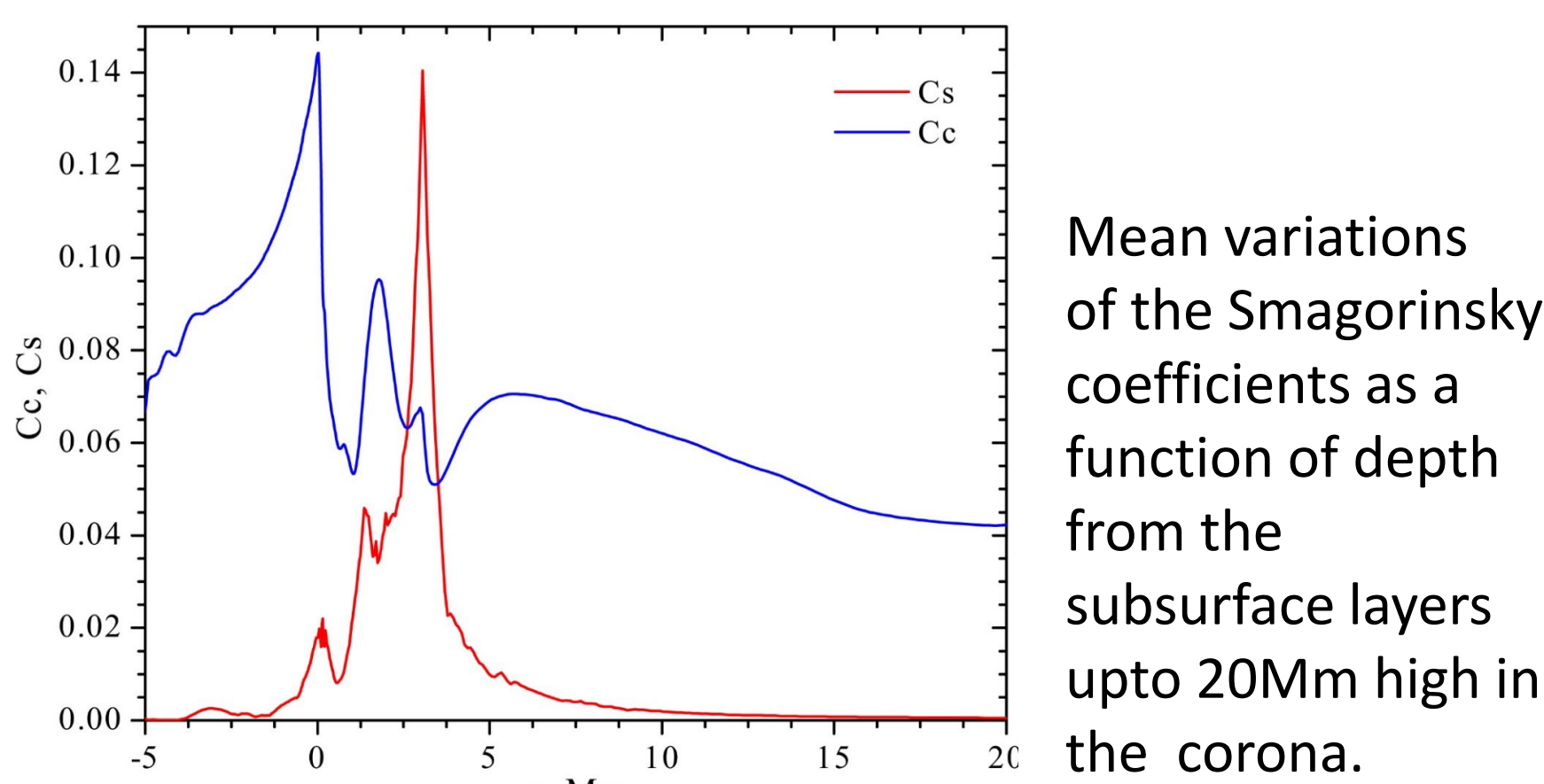
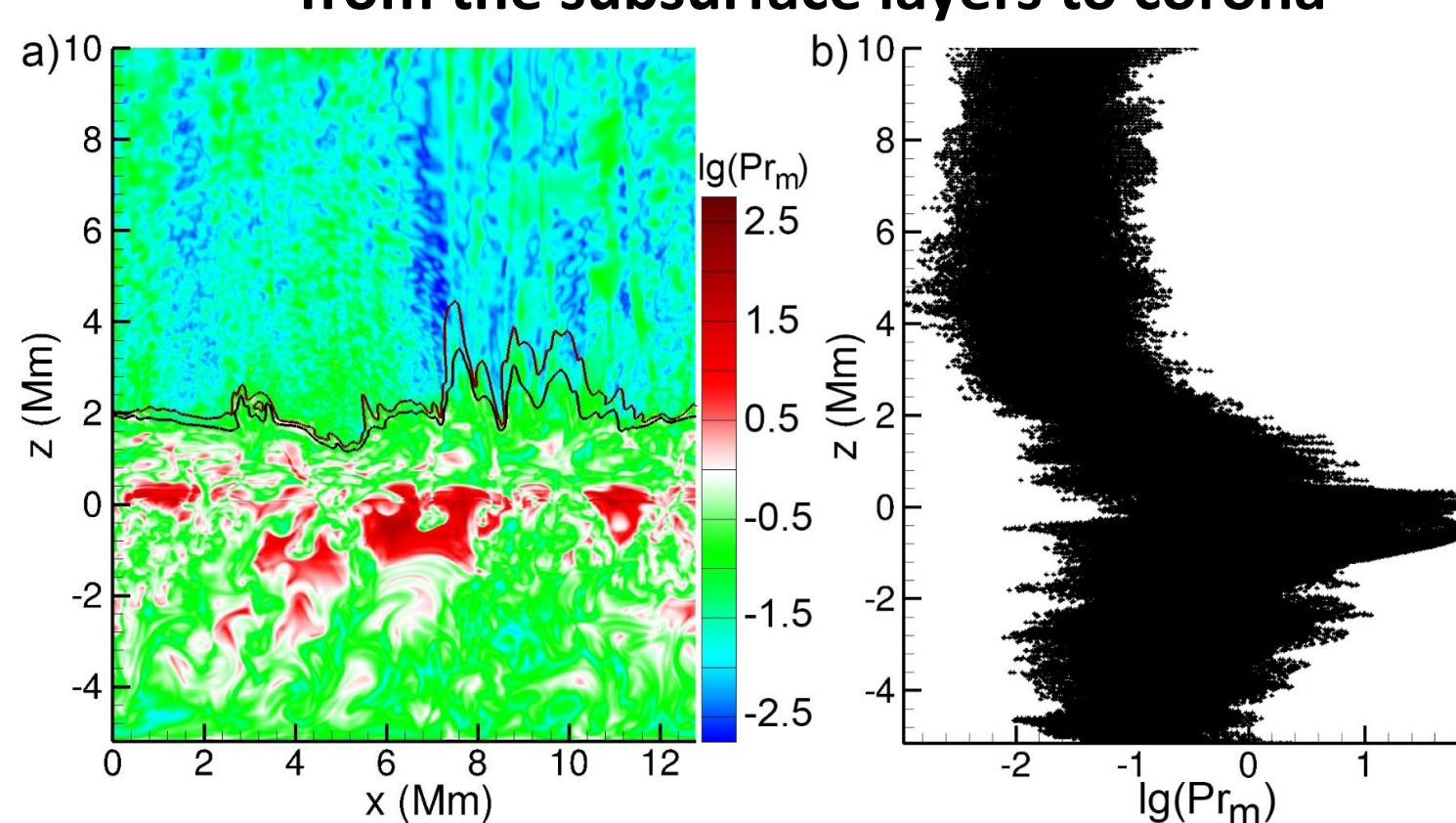


View through the solar atmosphere from the corona towards the transition zone and corona. The simulation results show a self-formed magnetic structure in the corona that is connected with kilogauss magnetic field in the photosphere through the chromosphere and transition zone. Visualization is performed by advecting particles seeded at height 2.4Mm above the solar surface.

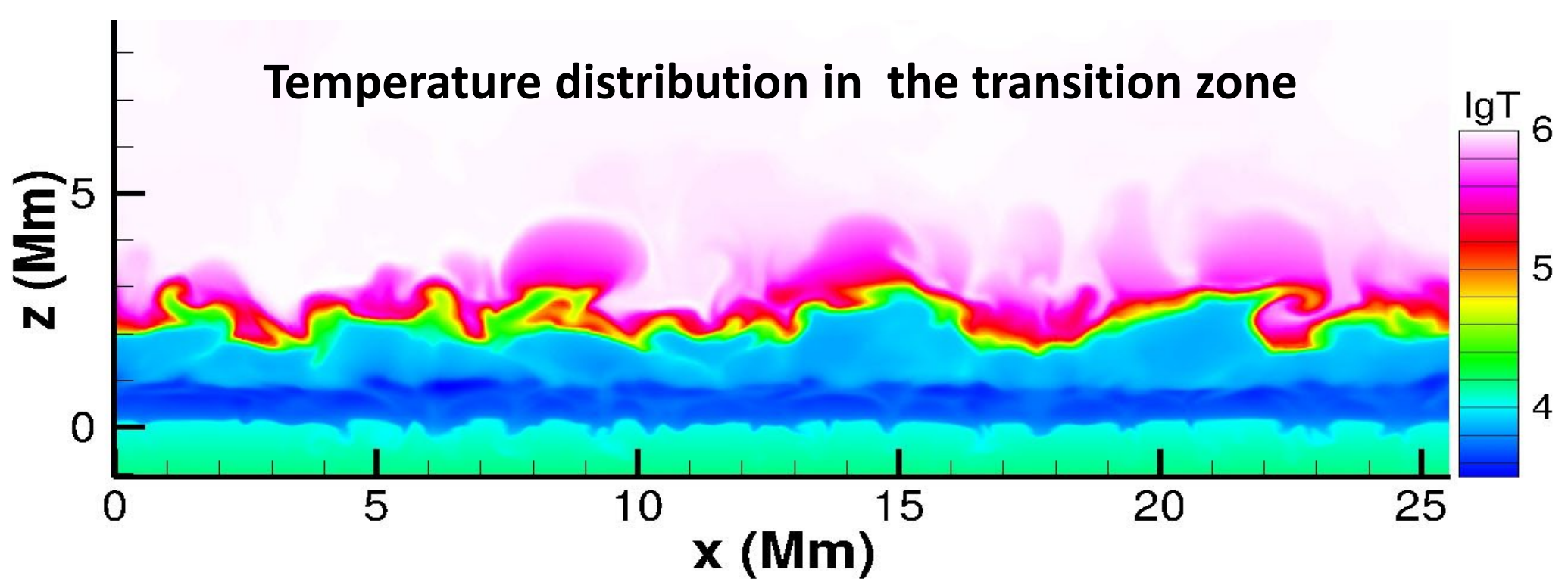
## Enstrophy transport from the transition zone to the corona



## Variations of the turbulent magnetic Prandtl number from the subsurface layers to corona

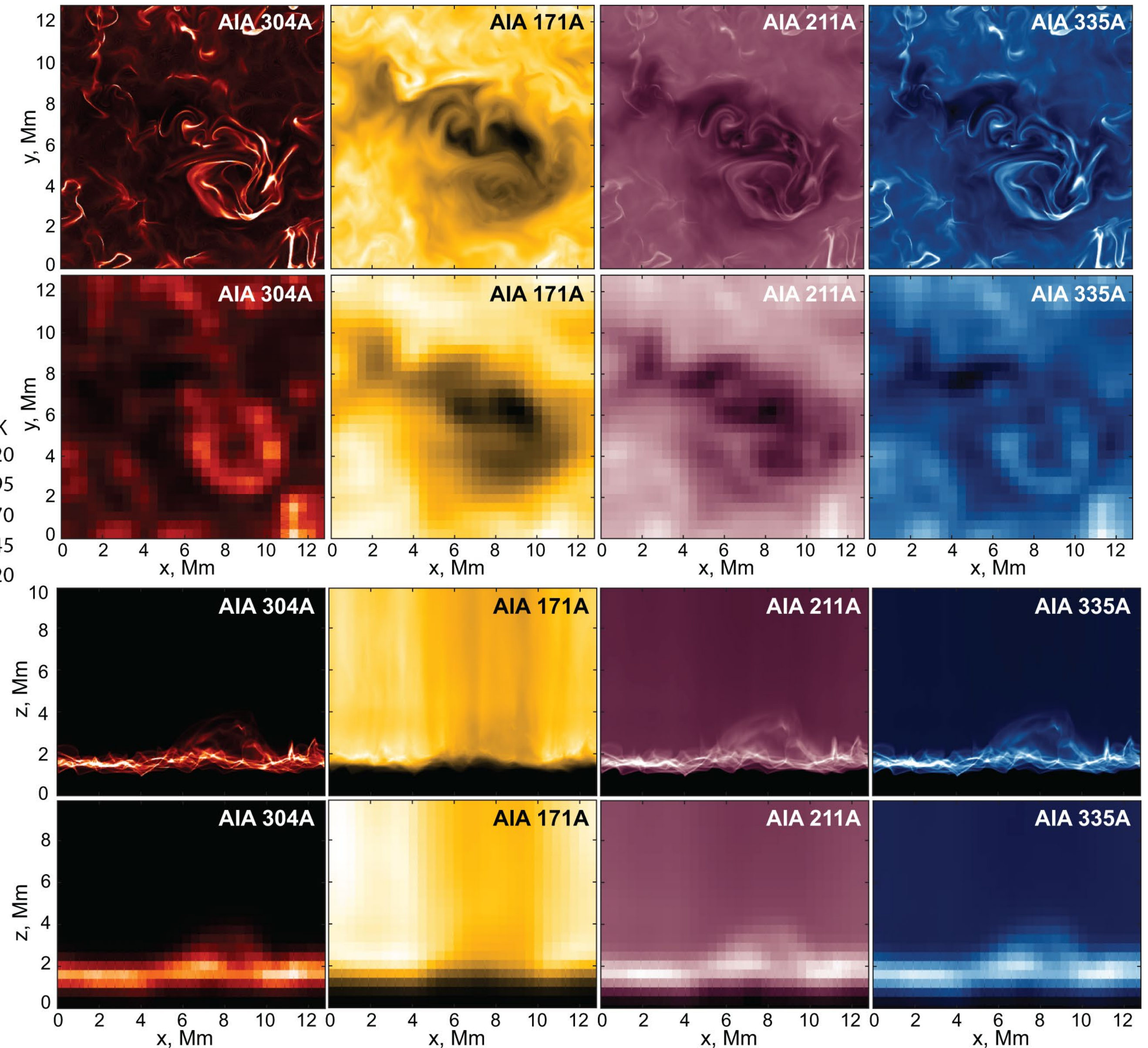


Distributions of a) vertical velocity, b) temperature, and c) magnetic field in a quiet Sun region at height 10~Mm above the photosphere. The vertical slice in panel d) shows propagation of high-frequency perturbations of divergence of the velocity from the transition zone to the upper layers of the corona. Color curves in panel d) correspond to temperatures of the transition region of 0.1MK and 0.5MK. Black streamlines with arrows indicate magnetic field lines. Kitiashvili et al., 2020.

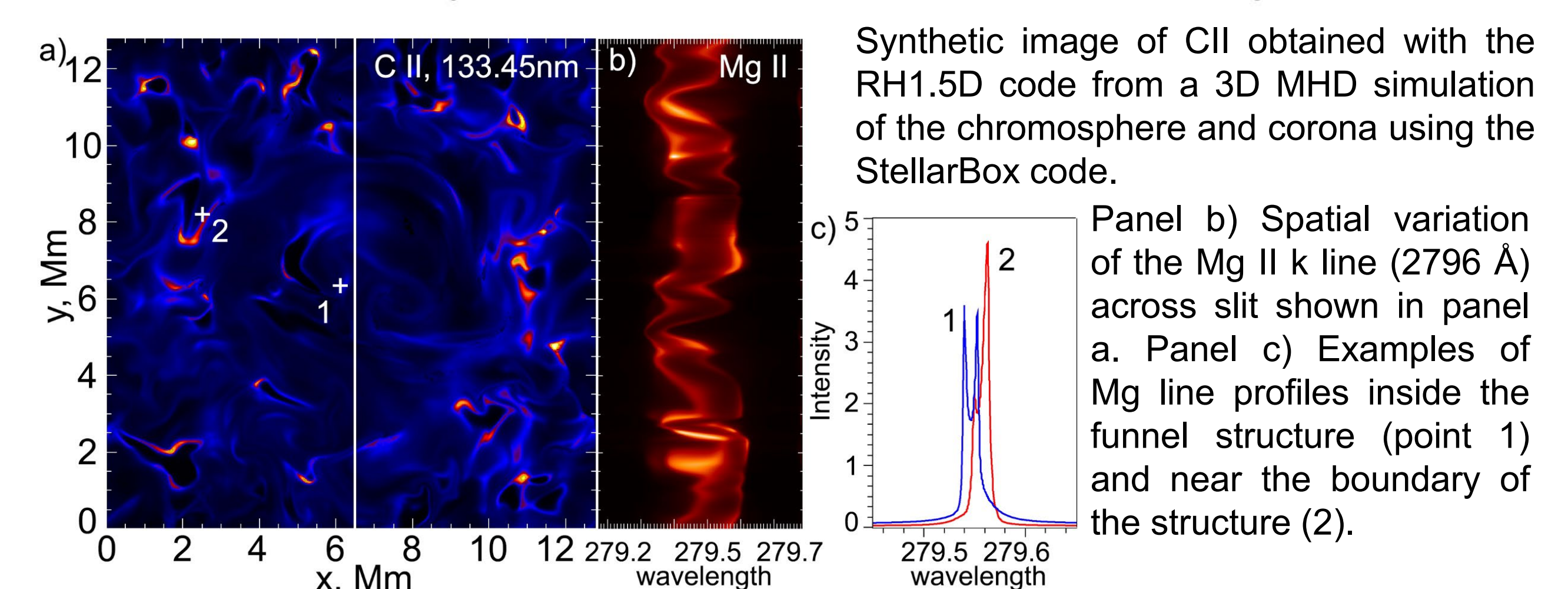
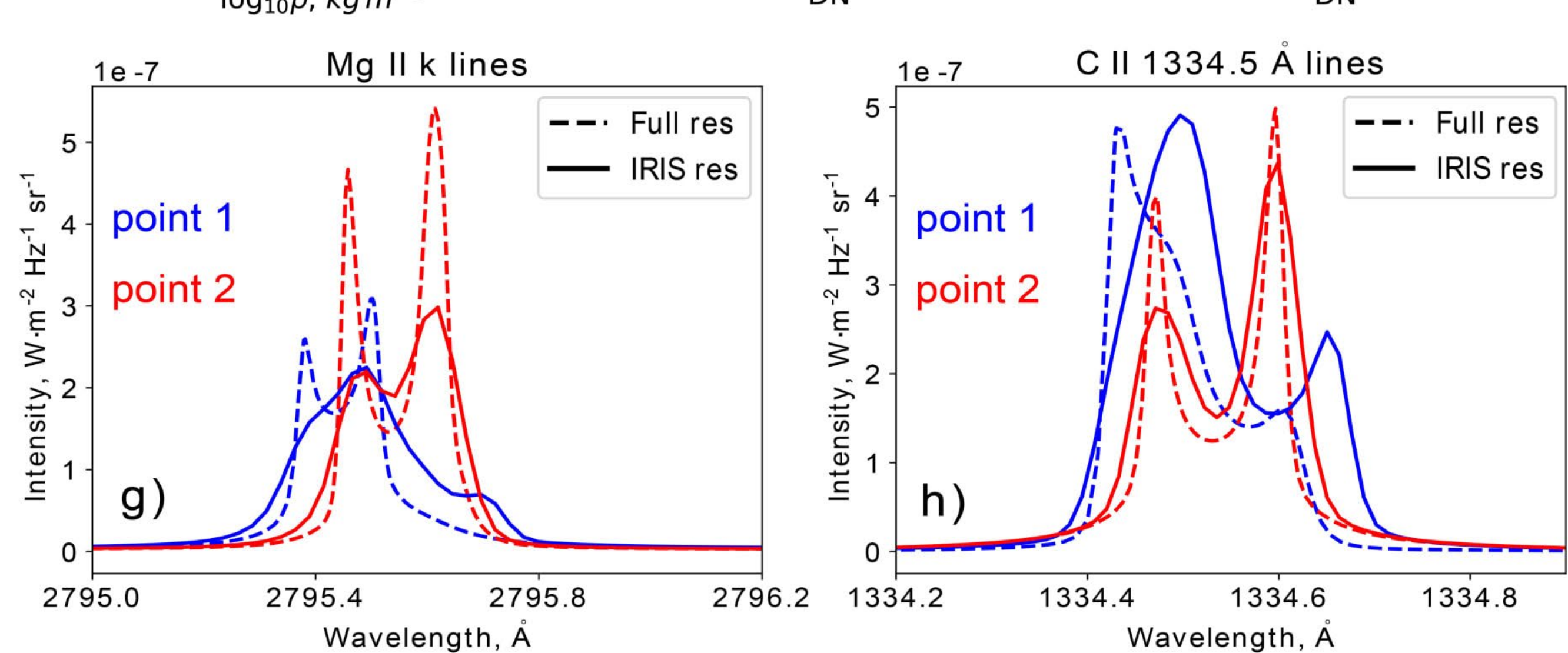
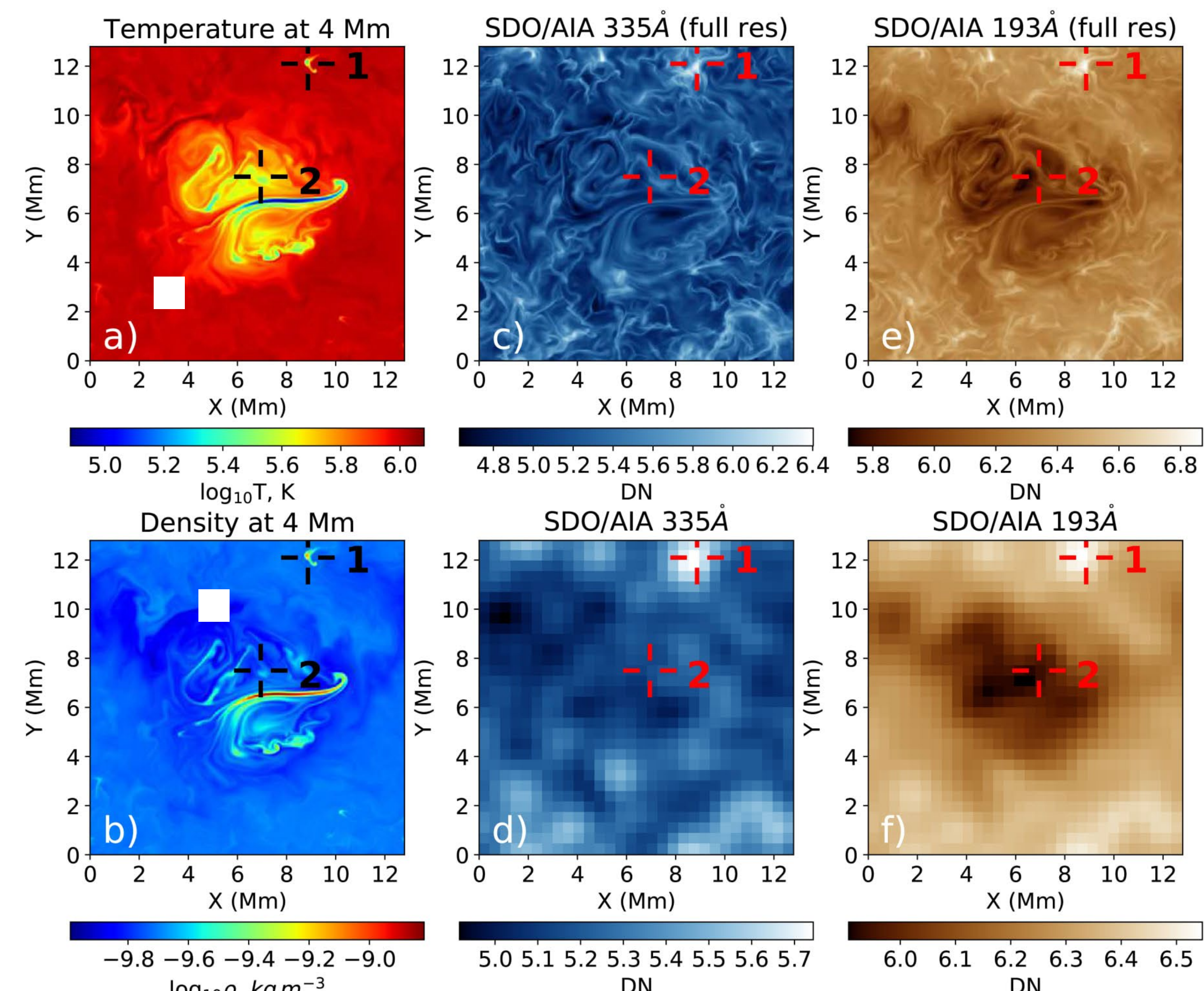


Evolution of a) the Mg II k line spectra, b) C II 1334.5A line spectra, c) normalized SDO/AIA emission, and d) physical parameters in the transition region (at the height corresponding to 5x10<sup>5</sup>K). The vertical dotted lines mark the time moments of the strongest SDO/AIA 335A emission during the shock. The vertical dotted lines mark the time moments of the Mg II k intensity peak (panel a), C II 1334.5A intensity peak (panel b), and SDO/AIA 304A peak (panel c). The dotted area in panel (d) indicates the positive enthalpy flux (Sadykov et al., 2021).

## Synthetic AIA emission in four channels calculated with the full numerical and instrumental resolution, and for two views at the disc center and the limb



Physical properties and synthetic emission at the starting time of the considered simulation series: a) temperature, and b) density distributions at 4Mm height; synthetic SDO/AIA 335A emission at c) computational, and d) instrumental resolutions; synthetic SDO/AIA 193A emission at e) computational and f) instrumental resolutions; g) Mg II k and h) C II 1334.5A line profiles derived in points 1 (blue) and 2 (red) at computational (dashed) and instrumental (solid) resolutions. Points 1 and 2 are marked by crosshairs in panels a-f (Sadykov et al., 2021).



## Conclusions

Solar coronal activity is the primary source of space weather disturbances. Realistic modeling of the corona is critical for understanding the origins of space weather and for predicting the impacts of solar activity on the near-Earth space environment. To investigate the underlying physical processes, we performed 3D radiative MHD simulations taking into account all essential physics and employing sub-grid scale turbulence models, thereby reproducing the local dynamo process, spontaneous flow eruptions, coronal structure, and dynamics in the quiet-Sun.

Analysis of synthetic data reveals sharp enhancements of the synthetic EUV emission Mg II spectral lines and Doppler velocity jumps. The Doppler velocity jumps in the C II 1334.5 A (IRIS line), and the relative enhancement of the 335 A emission (SDO/AIA) are the best proxies for the enthalpy deposited by shocks in the corona (the Kendall  $\tau$  correlation coefficients are 0.59 for 1334.5A and 0.38 for 335A).

It is found that the transition zone between the low temperature (10<sup>4</sup> K) chromosphere and hot (10<sup>6</sup> K) corona is substantially more turbulent and dynamic than previously assumed. The simulations reveal new processes of generation of shocks and plasma eruptions and show that the transition region dynamics is a source of the corona expansion and formation of the solar wind. Our simulations reveal that initially uniform weak magnetic fields are greatly amplified by small-scale dynamo below the Sun's visible surface and cause spontaneous formation of tornado-like plasma structures and eruptions above the surface. The strongest helical flows originate in strong kilogauss magnetic field patches formed on the solar surface. These helical magnetized structures extend into the corona, producing Alfvén waves that drive plasma eruptions. The simulations also reveal many important details unresolved in observational data, such as the Kelvin-Helmholtz instability of the magnetic structures and plasma downflows in the corona. The simulations reveal new processes of generation shocks and plasma eruptions and show that the transition region dynamics is a source of the corona expansion and formation of the solar wind.

Magnetic field concentrations with a field strength of about 1kG are strong enough to extend magnetized structures into the corona. The complexity of these structures increases with height and often shows splitting into substructures. In particular, helical patterns of various scales appear and disappear with time. The vertical velocity distribution is highly inhomogeneous and reveals strong upflows above 100km/s and downflows with ~10 km/s speed. Interestingly, during the formation and 'active' evolution of the magnetic structures, high complexity flows and numerous strong shocks are excited. Then, during the decay phase, the amplitudes of the fluctuations associated with shock waves decrease (Kitiashvili et al., 2020).